

Hydrogenation of Simple Aromatic Molecules: A Computational Study of the Mechanism

George Zhong, Bun Chan,* and Leo Radom*

*Contribution from the School of Chemistry and Centre of Excellence in Free Radical Chemistry
and Biotechnology, University of Sydney, Sydney, NSW 2006, Australia*

Received August 28, 2006; E-mail: chan_b@chem.usyd.edu.au; radom@chem.usyd.edu.au

Abstract: Quantum chemistry calculations have been used to study the metal-free hydrogenation reactions of a variety of simple aromatic, heteroaromatic, and related linear conjugated systems. We find that the barrier for uncatalyzed 1,4-hydrogenation is always substantially lower (by approximately 200 kJ mol⁻¹) than that for 1,2-hydrogenation, despite similar reaction enthalpies. The presence of hydrogen fluoride as a catalyst is found to decrease the 1,2-hydrogenation barriers but, in most cases, to slightly increase the 1,4-hydrogenation barriers when a constrained geometric arrangement is employed. These qualitative observations are consistent with orbital symmetry considerations, which show that both the uncatalyzed 1,4-hydrogenation and the catalyzed 1,2-hydrogenation are formally symmetry-allowed processes. An extreme example of the catalyzed 1,2-hydrogenation of benzene is provided by the involvement of a second molecule of hydrogen, which leads to a substantial lowering of the barrier. The effect of catalysis was further investigated by applying a selection of additional catalysts to the 1,2- and 1,4-hydrogenation of benzene. A decreasing barrier with increasing catalyst acidity is generally observed for the catalytic 1,2-hydrogenation, but the situation is more complex for catalytic 1,4-hydrogenation. For the uncatalyzed 1,4-hydrogenation of aromatic systems containing one or more nitrogen heteroatoms, the barriers for [C,C], [C,N], and [N,N] hydrogenations are individually related to the reaction enthalpies by the Bell–Evans–Polanyi principle. In addition, for a given reaction enthalpy, the barriers for [C,C] hydrogenation are generally lower than those for [C,N] or [N,N] hydrogenation. Finally, we find that the distortion experienced by the reactants in forming the transition structure represents a secondary factor that influences the reaction barrier. The correlation between these quantities allows the 1,4-hydrogenation barriers to be predicted from a ground-state property.

1. Introduction

Hydrogenation is an important chemical reaction in industrial and biological processes. Most hydrogenation reactions are catalyzed by transition-metal complexes, both in laboratory synthesis¹ and in biological systems.² For example, compounds that contain platinum-group metals have been used extensively in the hydrogenation of fats in the food industry.³ In contrast to transition-metal-catalyzed hydrogenations, uncatalyzed hydrogenation and catalytic hydrogenation without transition metals are much less prominent. Among studies of such reactions, much attention has been devoted to uncatalyzed thermolysis reactions of organic compounds under H₂ due to

their relevance to coal liquefaction processes.⁴ These reactions usually proceed via radical mechanisms that involve H atoms. On the other hand, it has been shown that anthracene undergoes uncatalyzed hydrogenation in a one-step process.⁵ In the area of transition-metal-free catalytic hydrogenation, it has been found experimentally that strong acids or bases can be used as catalysts for the hydrogenation of unsaturated hydrocarbons and carbonyl compounds.⁶ It has also been demonstrated that zeolites catalyze the hydrogenation of alkenes.⁷

As part of a continuing investigation,⁸ we have been interested in pursuing the fundamentals of transition-metal-free hydrogenation. In one of these studies,^{8d} we found that in the acid-catalyzed

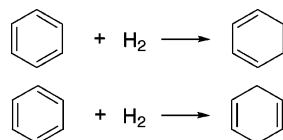
- (1) For example, see: (a) Rylander, P. N. *Hydrogenation over Platinum Metals*; Academic Press: New York, 1967. (b) Jacobsen, E. N., Pfaltz, A., Yamamoto, H., Eds.; *Comprehensive Asymmetric Catalysis*; Springer: Berlin, 1999; Vol. 1. (c) Nishimura, S. *Handbook of Heterogeneous Catalytic Hydrogenation for Organic Synthesis*; Wiley: New York, 2001. (d) Genet, J.-P. *Acc. Chem. Res.* **2003**, *36*, 908.
- (2) For general reviews on hydrogenases, see: (a) Albracht, S. P. J. *Biochim. Biophys. Acta* **1994**, *1188*, 167. (b) Ermiler, U.; Grabarse, W.; Shima, S.; Goubeaud, M.; Thauer, R. K. *Curr. Opin. Struct. Biol.* **1998**, *8*, 749. (c) Evans, D. J.; Pickett, C. J. *Chem. Soc. Rev.* **2003**, *32*, 268.
- (3) For example, see: (a) Baltes, J.; Cornils, B.; Frohning, C. D. *Chem.-Ing.-Tech.* **1975**, *47*, 522. (b) Cecchi, G.; Ucciani, E. *Riv. Ital. Sostanze Grasse* **1979**, *56*, 235. (c) Plourde, M.; Belkacemi, K.; Arul, J. *Ind. Eng. Chem. Res.* **2004**, *43*, 2382.

- (4) For a recent review, see: Guthrie, R. D. *J. Anal. Appl. Pyrolysis* **2000**, *54*, 89.
- (5) Rajagopal, V.; Guthrie, R. D.; Shi, B.; Davis, B. H. *Prepr. Pap. Am. Chem. Soc., Div. Fuel Chem.* **1994**, *39*, 673.
- (6) (a) Walling, C.; Bollyky, L. *J. Am. Chem. Soc.* **1961**, *83*, 2968. (b) Walling, C.; Bollyky, L. *J. Am. Chem. Soc.* **1964**, *86*, 3750. (c) Siskim, M. *J. Am. Chem. Soc.* **1974**, *96*, 3641. (d) Berkessel, A.; Schubert, T. J. S.; Müller, T. N. *J. Am. Chem. Soc.* **2002**, *124*, 8693.
- (7) (a) Sano, T.; Hagiwara, H.; Okabe, K.; Okado, H.; Saito, K.; Takaya, H. *Sekiyu Gakkaiishi* **1986**, *29*, 89. (b) Bader, R. R.; Baumeister, P.; Blaser, H.-U. *Chimia* **1996**, *50*, 99.
- (8) (a) Scott, A. P.; Golding, B. T.; Radom, L. *New J. Chem.* **1998**, 1171. (b) Senger, S.; Radom, S. *J. Phys. Chem. A* **2000**, *104*, 7375. (c) Senger, S.; Radom, L. *J. Am. Chem. Soc.* **2000**, *122*, 2613. (d) Chan, B.; Radom, L. *Aust. J. Chem.* **2004**, *57*, 659. (e) Chan, B.; Radom, L. *J. Am. Chem. Soc.* **2005**, *127*, 2443.

hydrogenation of ethene, the reactivity increases as the catalyst becomes more acidic. In addition, the proton affinity is also important in influencing the activity of some of the catalysts. In the present paper, we extend our investigation to the hydrogenation of benzene and related heteroaromatic systems. We employ quantum chemistry computations to study the uncatalyzed and acid/base-catalyzed hydrogenation of such molecules, with the aim of gaining a better understanding of transition-metal-free hydrogenation processes.

2. Computational Methods

Standard *ab initio* molecular orbital theory and density functional theory calculations⁹ were carried out with the GAUSSIAN 03 program.¹⁰ Initial calculations were carried out to determine a suitable level of theory for the optimization of geometries, including an examination of the effect of this choice on high-level single-point energies. This involved obtaining the geometries of the reactants, transition structures, and products at the B3-LYP/6-31G(d), B3-LYP/6-31+G(d), B3-LYP/6-31++G(d), and B3-LYP/6-31+G(d,p) levels for the following reactions:



We find that the inclusion of diffuse functions on carbon can have a significant effect (up to 0.15 Å, 4.8°), but inclusion of polarization and diffuse functions on hydrogen generally results in smaller changes in geometries (<0.05 Å, <2.2°). Calculations at the G3(MP2)-RAD level¹¹ with the B3-LYP/6-31G(d), B3-LYP/6-31+G(d), and B3-LYP/6-31+G(d,p) geometries show that inclusion of polarization functions on hydrogen in the geometry optimization also does not contribute significantly to the absolute values of the single-point energies (Supporting Information Table S1). These results support our use of B3-LYP/6-31+G(d) geometries in the calculation of barriers.

Further calculations were carried out to evaluate the accuracy of barriers and reaction enthalpies obtained with MPWB1K¹² with the 6-311+G(3df,2p) basis set, through comparison with high-level G3(MP2)-RAD values. The barriers and reaction enthalpies for both the uncatalyzed and HF-catalyzed 1,2- and 1,4-hydrogenation of benzene were calculated at the two levels of theory (Supporting Information Table S2). We find that MPWB1K/6-311+G(3df,2p) gives good agreement with G3(MP2)-RAD for reaction enthalpies. The predicted barriers are not quite as good, being underestimated by up to 15 kJ mol⁻¹, but this is fairly consistent across the four reactions examined. On the basis of these results, we have used the computationally cost-effective MPWB1K/6-311+G(3df,2p) method with B3-LYP/6-31+G(d) geometries in the calculation of barriers and reaction enthalpies.

Unless otherwise noted, B3-LYP/6-31+G(d) zero-point vibrational energies (ZPVEs) were incorporated into all reported barriers and reaction enthalpies. Literature scaling factors¹³ were used in the evaluation of the zero-point energies (0.9806) and thermal energies (0.9989) from the B3-LYP/6-31+G(d) harmonic vibrational frequencies.

- (9) For example, see: (a) Hehre, W. J.; Radom, L.; Schleyer, P. v. P.; Pople, J. A. *Ab Initio Molecular Orbital Theory*; Wiley: New York, 1986. (b) Jensen, F. *Introduction to Computational Chemistry*, 2nd ed.; Wiley: Chichester, 2007. (c) Koch, W.; Holthausen, M. C. *A Chemist's Guide to Density Functional Theory*, 2nd ed.; Wiley: New York, 2001.
- (10) Frisch, M. J., et al. *Gaussian 03*, revision B.03; Gaussian, Inc.: Pittsburgh, PA, 2003.
- (11) (a) Henry, D. J.; Sullivan, M. B.; Radom, L. *J. Chem. Phys.* **2001**, *118*, 4849. (b) Henry, D. J.; Parkinson, C. J.; Mayer, P. M.; Radom, L. *J. Phys. Chem. A* **2001**, *105*, 6750. (c) Henry, D. J.; Sullivan, M. B.; Radom, L. *J. Chem. Phys.* **2003**, *118*, 4849.
- (12) Zhao, Y.; Truhlar, D. G. *J. Phys. Chem. A* **2004**, *108*, 6908.
- (13) Scott, A. P.; Radom, L. *J. Phys. Chem.* **1996**, *100*, 16502.

Table 1. Barriers (0 K, kJ mol⁻¹) for Uncatalyzed and HF-Catalyzed Hydrogenation Reactions^a

substrate	uncatalyzed barrier		catalyzed barrier	
	1,2	1,4	1,2	1,4
ethene	343		228	
formaldehyde	268 ^b		130 ^b	
benzene	424	219	313	289
1,3-butadiene ^c	345	135	241	212
acrolein ^c	354	152 ^b	222	128 ^b
glyoxal ^c	280 ^b	211 ^e	157 ^b	237 ^e
propenimine ^c	353	130 ^d	233	104 ^d
cyclopentadiene	368	145	236	220
furan	391	181	267	239
pyrrole	387	205	258	223
thiophene	412	214	275	261

^a All hydrogenations are of the [C,C] type unless otherwise noted. ^b [C,O] hydrogenation. ^c Barriers obtained for constrained *cis* structures. ^d [C,N] hydrogenation. ^e [O,O] hydrogenation.

The intrinsic reaction coordinate (IRC) method was employed to confirm that each transition structure is linked to the appropriate adjacent minima. All geometrical parameters in the text refer to B3-LYP/6-31+G(d) values, while relative energies are MPWB1K/6-311+G(3df,2p)/B3-LYP/6-31+G(d) values in the gas phase at 0 K, unless otherwise noted. Population analyses were carried out at the B3-LYP/6-311+G(3df,2p) level using the natural bond orbital (NBO) method.¹⁴

3. Results and Discussion

3.1. Overview. The barriers for the 1,2- and 1,4-hydrogenations of a broad selection of molecules were calculated in the present study in order to gain insight into their respective mechanisms. The effectiveness of catalysis on both types of hydrogenation was initially investigated using a representative acid catalyst, namely hydrogen fluoride. Table 1 presents the 1,2- and 1,4-hydrogenation barriers, both with and without HF catalysis, for the set of molecules studied. We can see that the uncatalyzed 1,4-hydrogenation barrier is substantially smaller than the corresponding uncatalyzed 1,2-hydrogenation barrier in all cases. This is consistent with experimental observations in the case of benzene that the reverse of the uncatalyzed hydrogenation reaction, namely the dehydrogenation reactions of 1,3-cyclohexadiene and 1,4-cyclohexadiene, have substantially different temperature requirements.^{15,16} Thus, while the concerted dehydrogenation of 1,4-cyclohexadiene proceeds at a relatively moderate temperature of 300 °C,¹⁵ the corresponding unimolecular dehydrogenation of 1,3-cyclohexadiene is not competitive with alternative radical and biradical mechanisms, even under very low pressure and at a temperature above 700 °C.¹⁶

The differences between the barriers for the 1,2- and 1,4-hydrogenation reactions lie within the relatively narrow range 200 ± 25 kJ mol⁻¹, with values varying from 182 kJ mol⁻¹ (pyrrole) to 223 kJ mol⁻¹ (cyclopentadiene). Interestingly, acid catalysis (see, for example, Figure 1a) is generally beneficial for 1,2-hydrogenation reactions, but it is unfavorable for 1,4-hydrogenation reactions in which a constrained geometric

- (14) (a) Foster, J. P.; Weinhold, F. *J. Am. Chem. Soc.* **1980**, *102*, 7211. (b) Reed, A. E.; Weinhold, F. *J. Chem. Phys.* **1983**, *78*, 4066. (c) Reed, A. E.; Weinstock, R. B.; Weinhold, F. *J. Chem. Phys.* **1985**, *83*, 735.
- (15) Benson, S. W.; Shaw, R. *Trans. Faraday Soc.* **1967**, *63*, 985.
- (16) (a) Alfassi, Z. B.; Benson, S. W.; Golden, D. M. *J. Am. Chem. Soc.* **1973**, *95*, 4784. (b) Orchard, S. W.; Thrush, B. A. *J. Chem. Soc., Chem. Commun.* **1973**, 14.



Figure 1. Transition structures for (a) the HF-catalyzed 1,2-hydrogenation of ethene and (b) the HF-catalyzed 1,4-hydrogenation of 1,3-butadiene showing the constrained geometric arrangement employed.

arrangement (see, for example, Figure 1b) is employed.¹⁷ We find that HF catalysis of 1,2-hydrogenation lowers the barrier by approximately 120 kJ mol⁻¹. Contrastingly, HF catalysis is found to increase the barrier for 1,4-hydrogenation by up to 80 kJ mol⁻¹.

3.2. Hydrogenation of Benzene. 3.2.1. Orbital Symmetry Considerations. We can regard the 1,4-hydrogenations as [4 + 2]-type reactions, corresponding to the interaction of four benzene π -orbitals (4 electrons) with two hydrogen σ -orbitals (2 electrons). Similarly, we can regard the 1,2-hydrogenations as [6 + 2]-type reactions where six benzene π -orbitals (6 electrons) interact with two hydrogen σ -orbitals (2 electrons). Treating the reactions in this manner enables the trends in the hydrogenation barriers to be qualitatively rationalized using orbital symmetry considerations (Figure 2).¹⁸ The orbital correlation diagram clearly shows that the 1,4-hydrogenation is formally symmetry allowed and might be expected to have a lower barrier, while the 1,2-hydrogenation is symmetry forbidden and might be expected to have a higher barrier.¹⁹

Extending this description further, the thermally forbidden 1,2-hydrogenation reactions ([6 + 2]-type) can be assisted by the presence of a catalyst (HX), which creates a thermally allowed [6 + 2 + 2] reaction and, hence, leads to a lowering of the reaction barrier. In contrast, the presence of a catalyst in thermally allowed 1,4-hydrogenations ([4 + 2]-type) hinders the reaction by converting the symmetry-favored reaction pathway to one that is formally symmetry-forbidden ([4 + 2 + 2]-type).¹⁷

In the 1,4-hydrogenation of acrolein and propenimine, the presence of heteroatoms lowers the overall symmetry of the system, and hence the orbital symmetry considerations are less significant in these cases. Thus, one might expect a narrowing of the gap between the barriers for the uncatalyzed and (constrained) catalyzed reactions compared with that for 1,3-butadiene. In fact, HF catalysis in these cases goes one step further and actually *facilitates* the 1,4-hydrogenation of acrolein and propenimine, indicating that there is an additional favorable factor contributing to these reactions. The lower barrier may be associated with the lower symmetry of the substrates, leading to a less synchronous reaction, which is more favored by acid catalysis. Another possible explanation comes by recognizing that these substrates possess a dipole moment, and there may

be stabilization of the transition structures through dipole–dipole interactions with the HF catalyst.

In the following sections, we attempt to investigate in more detail the relationship between the orbital interactions and the observed preferences among the four hydrogenation pathways described above. We use benzene as the initial model substrate in our studies owing to its simplicity. Calculations of the overall reaction enthalpy for the hydrogenation of benzene indicate that both the 1,2-hydrogenation (leading to 1,3-cyclohexadiene) and the 1,4-hydrogenation (leading to 1,4-cyclohexadiene) of benzene are endothermic, with reaction enthalpies (298 K) of 30.2 and 30.9 kJ mol⁻¹, respectively (G3(MP2)-RAD, Supporting Information Table S1).²⁰ These results are slightly higher than the corresponding experimental values of 21.7 and 21.9 kJ mol⁻¹, respectively.^{20,21} The small difference in reaction enthalpies, arising because of the almost equal energies of 1,3-cyclohexadiene and 1,4-cyclohexadiene, indicates that thermodynamics is not responsible for the substantial differences in the calculated barriers.

3.2.2. 1,2-Hydrogenation. The 1,2-hydrogenation reaction was studied in detail, with a focus on the 1,2-hydrogenation of benzene to afford 1,3-cyclohexadiene. Figure 3 depicts the optimized geometry of the transition structure for this reaction. The two reacting H atoms are not equivalent, with one of them lying significantly closer to the benzene ring (C··H = 1.370 Å) than the other (C··H = 1.547 Å). This is similar to the situation for the transition structure for ethene hydrogenation.^{8d} The difference in the nature of the two H atoms is further indicated by NBO population analysis, which shows the development of charge separation across the two H atoms in the transition structure. It appears from the NBO analysis that the protonation of a benzene CC bond is more advanced than the concomitant hydride addition at the adjacent site.

The resulting distorted parallelogram geometry reflects the forbidden nature of thermal [2 + 2]-type reactions, whereby a symmetrical rectangular transition structure is not allowed. It has previously been proposed²² that such a distorted structure could allow more effective orbital interactions for otherwise forbidden [2 + 2]-type reactions. We find that a distorted parallelogram geometry is, in fact, also observed for many of the other 1,2-hydrogenation reactions (listed in Table 1). One specific example is the 1,2-hydrogenation of *cis*-1,3-butadiene, where the optimized transition structure (Figure 4) shows similar features to those noted in the TS for the 1,2-hydrogenation of benzene (Figure 3). The two reacting hydrogen atoms that constitute the parallelogram geometry are again noticeably different, with one hydrogen atom significantly closer to the butadiene substrate than the other. The NBO analysis again shows that the hydrogen atom that is closer to the butadiene substrate is significantly more positively charged than its counterpart.

3.2.3. 1,2-Catalytic Hydrogenation. As noted above, the 1,2-hydrogenation reactions benefit from the presence of an acid catalyst. We have studied this aspect in detail for the 1,2-

(17) The fact that such catalysis leads to an increased barrier in most cases of course implies that in reality the reaction is not likely to utilize the catalyst in this way but would proceed either in an uncatalyzed manner or with the “catalyst” in almost a spectator role. Nonetheless, the lower barriers observed in some cases demonstrate the subtleties in such catalytic reactions. The purpose of our calculations is to illustrate what happens in a constrained situation so as to indicate the fundamental principles at work and, thus, provide insights into the design of potential catalysts for such reactions.

(18) For example, see: (a) Woodward, R. B.; Hoffmann, R. *The Conservation of Orbital Symmetry*; Verlag Chemie: Weinheim, 1970. (b) Anh, N. *The Woodward-Hoffmann Rules*, 2nd ed.; McGraw-Hill: New York, 1980. (c) Fleming, I. *Pericyclic Reactions*; Oxford University Press: Oxford, 1999. (d) David, C. W. *J. Chem. Educ.* **1999**, *76*, 999. (e) Patterson, R. T. *J. Chem. Educ.* **1999**, *76*, 1002.

(19) In a simplified treatment, the 1,2-hydrogenation may be regarded as a [2 + 2]-type reaction, which is also symmetry forbidden.

(20) For comparison, the MPWB1K/6-311+G(3df,2p)//B3-LYP/6-31+G(d) reaction enthalpies are 26.6 and 25.4 kJ mol⁻¹, respectively.

(21) Calculated using $\Delta_f H_{298}$ values of benzene, 1,3-cyclohexadiene, and 1,4-cyclohexadiene from the NIST Chemistry Webbook (Linstrom P. J., Mallard W. G., Eds. *NIST Chemistry WebBook, NIST Standard Reference Database Number 69*; National Institute of Standards and Technology: Gaithersburg, MD 20899, June 2005 (<http://webbook.nist.gov>)).

(22) Zimmerman, H. E. *Acc. Chem. Res.* **1972**, *5*, 393.

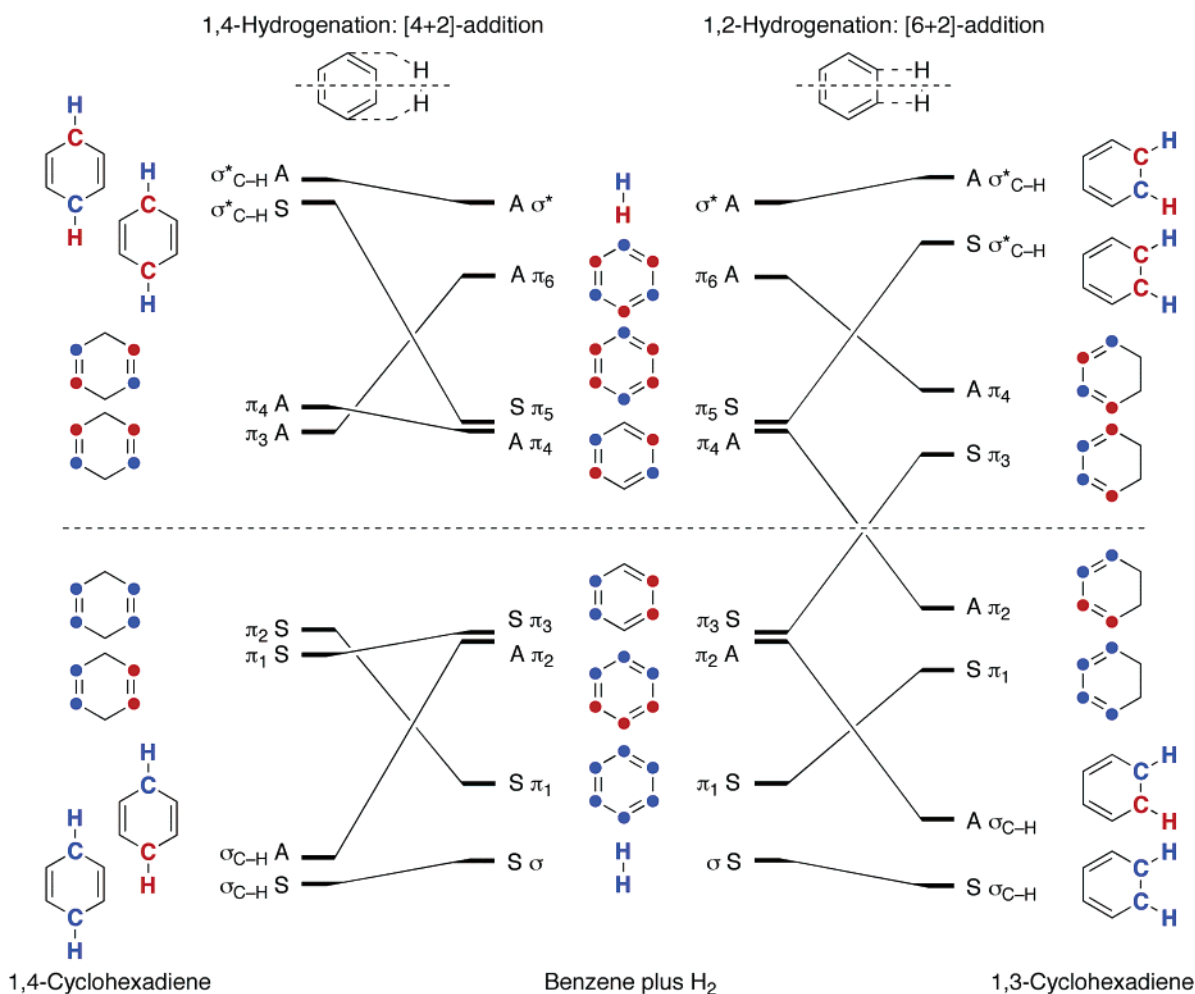


Figure 2. Orbital correlation diagrams for the 1,4- and 1,2-hydrogenation of benzene. Note that the orbitals labeled $\sigma_{\text{C-H}}$ and $\sigma^*_{\text{C-H}}$ in 1,4- and 1,3-cyclohexadiene have overall π symmetry.

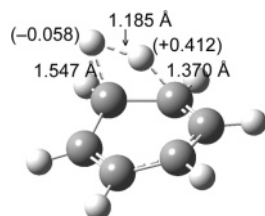


Figure 3. Transition structure for the uncatalyzed 1,2-hydrogenation of benzene. NBO charges of the two reacting hydrogen atoms are shown in parentheses.

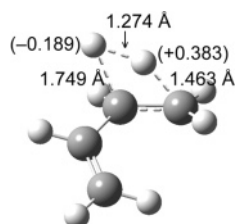


Figure 4. Transition structure for the uncatalyzed 1,2-hydrogenation of *cis*-1,3-butadiene. NBO charges for the two reacting hydrogen atoms are shown in parentheses.

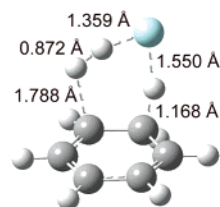


Figure 5. Transition structure for the HF-catalyzed 1,2-hydrogenation of benzene.

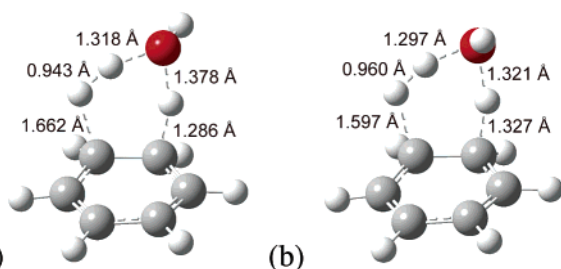


Figure 6. (a) Exo- and (b) endo-transition structures for the H₂O-catalyzed hydrogenation of benzene.

hydrogenation of benzene in the presence of a variety of common acid catalysts. The transition structure for the HF-catalyzed 1,2-hydrogenation of benzene is shown in Figure 5 as a representative example. For catalysts more complex than

HF, the nonhydrogenic component of the catalyst can point either into (denoted endo) or out from (denoted exo) the aromatic ring (as illustrated in Figure 6 for the case of H₂O). Our calculations show that the exo geometry gives rise to a slightly

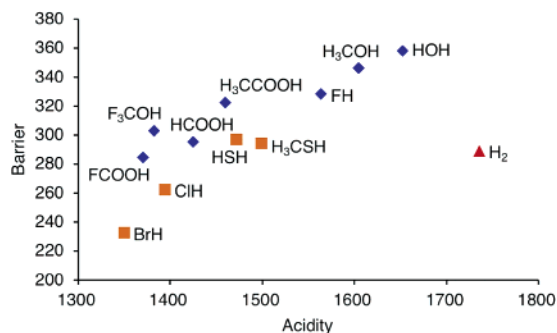


Figure 7. Calculated barriers versus catalyst acidities (\blacktriangle H₂; \blacklozenge first row; \blacksquare second or third row) for the catalytic 1,2-hydrogenation of benzene (0 K, kJ mol⁻¹).

lower barrier (differences less than 10 kJ mol⁻¹) for each catalyst examined, and hence we only report barriers corresponding to the exo geometry. We note that in the exo TS (Figure 6a), all the geometric parameters are closer to the parameters for the HF-catalyzed TS (Figure 5) than are the parameters for the endo TS (Figure 6b), e.g., a closer approach of the catalytic proton to the benzene ring.

Figure 7 shows a plot of the calculated barriers associated with the various catalysts versus their acidities. The gas-phase acidity values correspond to the calculated MPWB1K/6-311+G-(3df,2p)//B3-LYP/6-31+G(d) enthalpies at 0 K for the corresponding deprotonation reaction: $HX \rightarrow H^+ + X^-$. Note that a more acidic catalyst corresponds to a smaller numerical value on the acidity scale.

The barriers for all the catalyzed 1,2-hydrogenations of benzene that we have examined are significantly lower than that for the uncatalyzed hydrogenation (426 kJ mol⁻¹), in agreement with qualitative predictions based on orbital symmetry considerations. A particularly striking case is the H₂-catalyzed 1,2-hydrogenation of benzene, with the transition structure shown in Figure 8. We might have expected on the basis of both the low acidity and the low proton affinity of H₂ that H₂-catalysis would have little effect on the barrier. In fact, we find that the barrier is lowered by a substantial 140 kJ mol⁻¹, reflecting the importance of orbital symmetry effects.²³ Remarkably, the barrier for this reaction is lower than those for many of the reactions with catalysts with significantly higher acidity.²⁴ The higher symmetry in the H₂-catalyzed hydrogenation enables a concerted synchronous reaction, which leads to better orbital overlap and a lower barrier. This contrasts with the acid-catalyzed reactions, which are quite asynchronous. For example, as we have seen for the HF-catalyzed 1,2-hydrogenation (Figure 5), the two C–H bonds that are being formed in the transition structure in that case have quite different lengths of 1.788 Å and 1.168 Å.

With the exception of the H₂-catalyzed reaction, we can see from Figure 7 that the barrier decreases as the catalyst becomes more acidic. In addition, catalysts containing first-row atoms alone are found to lead to noticeably higher barriers than

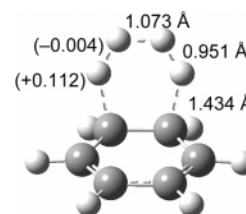


Figure 8. Transition structure for the H₂-catalyzed 1,2-hydrogenation of benzene. NBO charges for the two types of reacting hydrogen atoms are shown in parentheses.

catalysts with a similar acidity that include second- or third-row atoms. These trends are consistent with those previously observed in the catalytic hydrogenation of ethene.^{8d} The similarity in the trends for the two substrates suggests that the underlying factors that govern the catalytic 1,2-hydrogenation reactions for ethene and benzene are very similar and that, in both cases, a more acidic catalyst generally improves the catalytic ability.

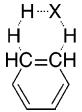
To further elucidate the relationship between the catalytic 1,2-hydrogenation of benzene and ethene, structural parameters for the transition structures for the catalyzed benzene hydrogenations have been examined. Table 2 lists selected bond lengths for the transition structures of interest, together with the calculated barriers and catalyst acidities. The structural parameters for the uncatalyzed hydrogenation of benzene are also included for comparison. We can see that for the catalysts containing only first-row atoms, the C \cdots HX and H \cdots H distances decrease while the CH \cdots X and X \cdots HH distances increase as the barrier becomes lower, which parallel the results previously obtained in the hydrogenation of ethene.^{8d} This agreement in the trends for the structural parameters provides a further indication that the catalyst influences the two 1,2-hydrogenation reactions in a similar way.

The calculated structures (Table 2) also indicate that the reaction becomes increasingly asynchronous as the catalyst becomes more acidic. For example, in the case of HBr (strong acid) catalysis, the calculated C \cdots HBr distance in the transition structure (1.142 Å) is only slightly longer than the corresponding C–H bond length in the resulting product (1.104 Å), 1,3-cyclohexadiene. The Br \cdots HH bond distance (1.989 Å), on the other hand, is significantly elongated compared with the Br \cdots H distance in hydrogen bromide (1.437 Å). We thus see from the relative bond lengths that protonation of the benzene ring by the hydrogen bromide catalyst has already proceeded almost to completion, while the degree of bond formation in the incipient HBr molecule is relatively modest. Hence, HBr-catalyzed 1,2-hydrogenation of benzene has a large carbocation character in the transition structure, with the catalyst creating a more ionic pathway that facilitates this reaction. The more ionic pathway is reflected in the NBO charges in the transition structure of +0.317 and -0.468 at the H atom (from HBr) and the Br atom, respectively, compared with the corresponding values of +0.203 and -0.203 in an isolated HBr molecule.

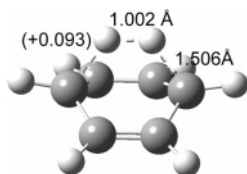
3.2.4. 1,4-Hydrogenation. We have also examined the 1,4-hydrogenation reaction in detail, with emphasis on the 1,4-hydrogenation of benzene, as well as simple aromatic systems involving nitrogen heteroatoms (see section 3.3). Figure 9 depicts the transition structure for the uncatalyzed 1,4-hydrogenation of benzene. It is evident that the transition

(23) We find that this effect is quite general: an additional molecule of H₂ substantially lowers the barrier for the uncatalyzed 1,2-hydrogenation of ethene and several other unsaturated substrates.

(24) We have carried out additional calculations on structures corresponding to HF complexed to the benzene or H₂ moieties of the TS of Figure 8, and the derived barrier is not significantly affected by the presence of HF; i.e., the HF molecule is effectively a spectator in these cases. The results in Figure 7 demonstrate the principles at work when the acid catalysts are more actively involved.

Table 2. Calculated Acidities and Barriers (0 K, kJ mol⁻¹) and Selected Structural Parameters (Å) for the Transition Structures Relevant to the Catalytic 1,2-Hydrogenation of Benzene


catalyst	acidity	barrier	C...HX	CH...X	X...HH	H...H	HH...C	C=C
uncatalyzed		426				1.185	1.370 1.547	1.503
HH	1735	289	1.434	0.951	1.073	0.951	1.434	1.458
HOH	1652	358	1.286	1.378	1.318	0.943	1.662	1.468
H₃COH	1604	347	1.263	1.405	1.314	0.936	1.699	1.468
FH	1563	328	1.168	1.550	1.359	0.872	1.788	1.473
H₃CCOOH	1459	323	1.123	1.956	1.560	0.828	1.810	1.479
F₃COH	1382	303	1.114	1.977	1.559	0.830	1.786	1.483
HCOOH	1424	296	1.118	2.023	1.577	0.825	1.812	1.481
FCOOH	1370	285	1.105	2.206	1.577	0.823	1.794	1.484
HSH	1471	294	1.179	2.057	1.911	0.844	1.703	1.477
H₃CSH	1499	294	1.191	2.000	1.876	0.853	1.693	1.477
CIH	1394	263	1.142	2.112	1.856	0.833	1.709	1.481
BrH	1349	233	1.142	2.216	1.989	0.834	1.669	1.483

**Figure 9.** Transition structure for the uncatalyzed 1,4-hydrogenation of benzene. The NBO charge on each atom of the reacting hydrogen molecule is shown in parentheses.

structure belongs to the C_{2v} point group, with the reacting pair of hydrogen atoms being equivalent. This contrasts with the transition structure for the 1,2-hydrogenation of benzene (Figure 3), where the reacting hydrogens are found to be nonequivalent. The structure is consistent with orbital symmetry considerations, with the overlap of the H_2 σ -orbital and a benzene π^* -orbital (τ_5), and the overlap of the H_2 σ^* -orbital and a benzene π -orbital (τ_2) being constructive in C_{2v} symmetry (see Figure 1).

Another striking feature of the transition structure is the amount of ring distortion that accompanies the addition of H_2 . We can see that two carbon atoms of the benzene ring are significantly displaced out of the aromatic plane, with the concomitant elongation of the dissociating H_2 bond, giving rise to a boat-like conformation. In comparison, the 1,2-hydrogenation reaction proceeds with far less ring distortion (Figure 3), with only minor half-chair-like puckering of the benzene ring found in the transition structure. This is consistent with ring-distortion-energy calculations (described in detail in section 3.3), which show that the 1,4-distortion energy, 186 kJ mol⁻¹, is 92 kJ mol⁻¹ larger than the 1,2-distortion energy, 94 kJ mol⁻¹; i.e., it requires considerably more energy to distort the benzene ring in the 1,4-hydrogenation than in the 1,2-hydrogenation. The extent of C–H bond formation in the 1,4-transition structure is noticeably less than that in the 1,2-transition structure, with C...H distances longer than 1.5 Å. This is probably associated with the greater distance required to be spanned by the reacting hydrogen atoms. Despite the larger ring distortion and less complete C–H bond formation, the barrier for the 1,4-hydrogenation of benzene is found to be lower than that for the 1,2-hydrogenation by more than 200 kJ mol⁻¹. This provides a

further indication that orbital symmetry is a dominating factor in determining the preferred hydrogenation pathway.

We find that other uncatalyzed 1,4-hydrogenation reactions, namely the reactions of various butadiene and cyclopentadiene derivatives (listed in Table 1), also have symmetric transition structures similar to that for the 1,4-hydrogenation of benzene (Figure 9). The two reacting hydrogens in the transition structure are equivalent in each case, being related by a plane of symmetry. The C...H bond-forming distance is also found to be greater than 1.5 Å in all cases. The many similarities in the transition structures suggest that the factors we find to govern the uncatalyzed 1,4-hydrogenation of benzene are likely to hold more generally for 1,4-hydrogenation of diene-type substrates.

All the 1,4-hydrogenation reactions discussed to this point involve reaction centers that are related by a plane of symmetry. We have also examined, though in somewhat less detail, 1,4-hydrogenation of substrates that have lower symmetry. The occurrence of nonidentical reaction centers can be classified into two types: the presence of substituents and the presence of ring-heteroatoms. In an attempt to study the effect of substituents on benzene hydrogenation, we have examined mono- and disubstituted benzene systems with π -electron-withdrawing groups (NO_2) and π -electron-donating groups (OH, NH_2) at various positions. We find that the presence of substituents increases the 1,4-hydrogenation barrier, regardless of the substitution pattern, but only to a small extent (by up to 10 kJ mol⁻¹, Supporting Information Table S4). In the case of substrates with heteroatom centers, namely acrolein and propenimine, the uncatalyzed 1,4-barriers are found to be 17 kJ mol⁻¹ higher and 5 kJ mol⁻¹ lower, respectively, than that for the 1,4-hydrogenation of 1,3-butadiene. Thus, the presence of nonidentical reaction centers appears to have only a minor effect on the reaction barrier.

3.2.5. 1,4-Catalytic Hydrogenation. In order to examine the effect of catalysis on the 1,4-hydrogenation reaction, we again chose to study in detail the model benzene system. Figure 10 illustrates the generic transition structure that we have examined

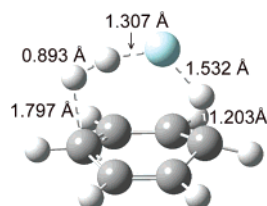


Figure 10. Transition structure for the HF-catalyzed 1,4-hydrogenation of benzene.

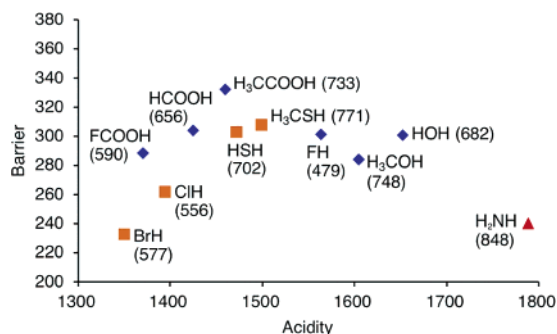


Figure 11. Calculated reaction barriers versus catalyst acidities (\blacktriangle H_2NH ; \blacklozenge first-row acids; \blacksquare second- or third-row acids) for the catalytic 1,4-hydrogenation of benzene (0 K, kJ mol^{-1}). Proton affinities of the catalysts are shown in parentheses.

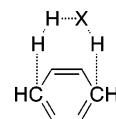
for the 1,4-hydrogenation of benzene in the presence of HF.²⁵ An immediate geometric difference with respect to the uncatalyzed reaction is that the presence of a catalyst lowers the molecular symmetry and the reaction becomes less synchronous. In addition, there is markedly less ring distortion relative to the uncatalyzed hydrogenation, as the catalyst reduces the distance required to be spanned by the reacting H_2 .

The barriers for the catalyzed 1,4-hydrogenation of benzene are plotted against the acidity of the corresponding catalyst in Figure 11. It can be seen that the barriers for the catalyzed 1,4-hydrogenations are all greater than the uncatalyzed 1,4-hydrogenation barrier of 219 kJ mol^{-1} , consistent with orbital symmetry considerations. As our calculations suggest that the application of catalysts in the 1,4-hydrogenation of benzene is not effective, we will only examine very briefly the underlying effects that influence the barrier.^{17,25}

A closer examination of Figure 11 reveals that the correlation between the hydrogenation barrier and the catalyst acidity, previously observed in the 1,2-catalyzed hydrogenations of both benzene (Figure 7) and ethene,^{8d} holds true only for the relatively more acidic catalysts. Furthermore, for these more acidic catalysts, we find that the energy difference between the catalyzed 1,4- and 1,2-barriers is less than 10 kJ mol^{-1} in each case. However, for the relatively less acidic catalysts (namely HOH, H_3COH , and FH), the difference in barriers for corresponding 1,2- and 1,4-catalyzed hydrogenations can be as much as 60 kJ mol^{-1} .

In order to help understand these observations, the structural parameters for the 1,4-catalyzed transition structures listed in Table 3 are compared with the corresponding 1,2-values of Table 2. We note that, for the first-row catalysts, the $\text{C}\cdots\text{HX}$ distance is generally longer for the corresponding 1,4-transition

Table 3. Calculated Acidities and Barriers (0 K, kJ mol^{-1}) and Selected Structural Parameters (\AA) for the Transition Structures Relevant to the Catalytic 1,4-Hydrogenation of Benzene



catalyst	acidity	barrier	$\text{C}\cdots\text{HX}$	$\text{CH}\cdots\text{X}$	$\text{X}\cdots\text{HH}$	$\text{H}\cdots\text{H}$	$\text{HH}\cdots\text{C}$
uncatalyzed		219				1.002	1.506
H_2NH	1788	260	2.038	1.057	1.191	1.148	1.417
HOH	1652	301	1.601	1.133	1.190	1.067	1.417
H_3COH	1604	285	1.682	1.091	1.162	1.097	1.399
FH	1563	302	1.203	1.532	1.307	0.893	1.797
H_3CCOOH	1459	332	1.164	1.769	1.510	0.844	1.846
HCOOH	1424	305	1.154	1.824	1.528	0.839	1.848
FCOOH	1370	289	1.138	1.950	1.494	0.846	1.786
H_3CSH	1499	308	1.113	2.547	1.975	0.810	2.010
HSH	1471	303	1.101	2.979	1.962	0.814	1.923
ClH	1394	262	1.123	2.474	1.886	0.818	1.882
BrH	1349	233	1.103	2.883	1.995	0.821	1.814

structures but the reverse is observed for the $\text{X}\cdots\text{HH}$ distance. This suggests that protonation by the catalyst is usually less complete for 1,4-systems relative to 1,2-systems. In the particular case of the weakly acidic HOH and H_3COH , the elongation in $\text{C}\cdots\text{HX}$ distances is found to be 0.274 \AA and 0.419 \AA , respectively. Such great differences in the $\text{C}\cdots\text{HX}$ distance suggest that acidity is not the governing factor in the 1,4-hydrogenation of benzene involving weakly acidic first-row catalysts. Furthermore, the $\text{X}\cdots\text{HH}$ and $\text{HH}\cdots\text{C}$ distances are relatively shorter for the 1,4-systems involving weakly acidic catalysts. This suggests that the proton affinity of the catalyst may be of greater importance than the acidity for these weakly acidic systems. Indeed, while H_3COH and H_2NH are among the least acidic first-row catalysts, their catalytic reactions have the lowest barriers for first-row catalysts, presumably due to their relatively high proton affinities.²⁶ This is consistent with our previous observation on acid-catalyzed hydrogenation of ethene,⁸ in which the barrier decreases as the proton affinity of the catalyst increases for weakly acidic catalysts.

Another feature readily observable from the structural parameters is that more acidic catalysts again give rise to less synchronous reactions, in a similar manner to the 1,2-catalyzed hydrogenation of benzene. For example, in the case of HBr catalysis, the $\text{C}\cdots\text{HBr}$ distance again closely resembles the $\text{C}\cdots\text{H}$ distance of the product, 1,4-cyclohexadiene, indicative of protonation being near completion, while the $\text{Br}\cdots\text{HH}$ distance is again significantly longer than the $\text{H}-\text{Br}$ distance of HBr, indicative of only partial proton re-abstraction from H_2 . It is likely that this similarity in mechanism gives rise to the observed similarities in the 1,4- and 1,2-catalyzed barriers for the more strongly acidic catalysts.

3.3. 1,4-Hydrogenation in Other Systems. The hydrogenation reactions examined to this point have mainly involved only carbon centers. For heteroaromatic systems such as pyridine, there is also the possibility of hydrogenation at a nitrogen atom. For example, 1,4-hydrogenation of pyridine at N1 and C4 can be regarded as the addition of hydrogen atoms to a nitrogen

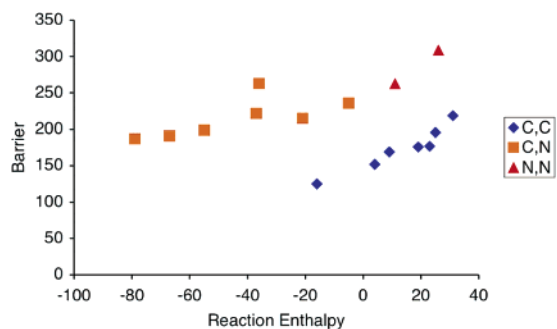
(25) Calculations on structures corresponding to HF complexed to the benzene or H_2 moieties of the uncatalyzed TS of Figure 9 show that the barrier (measured from the reactant complex) is only very slightly lowered from that for the uncatalyzed reaction.

(26) All proton affinities were computed at the G3(MP2)-RAD level and are taken from ref 8d with the exception of HBr, for which the proton affinity was computed as part of the present study.

Table 4. Calculated Barriers and Reaction Enthalpies (0 K, kJ mol⁻¹) and Selected Intramolecular Distances (Å) Relevant to the Uncatalyzed 1,4-Hydrogenation of Benzene and Related Heteroaromatic Systems

substrate	(X1,X2) ^a	type	<i>d</i> _{ring} ^b	X1...H ^c	X2...H ^c	X...H _{ave} ^d	H...H ^c	barrier	Δ <i>H</i> _{rxn}
benzene	1,4	[C,C]	2.797	1.506	1.506	1.506	1.002	219	31
pyridine	1,4	[C,N]	2.808	1.422	1.486	1.454	1.011	263	11
pyrimidine	2,5	[C,C]	2.729	1.507	1.527	1.517	0.980	196	25
	1,4	[C,N]	2.735	1.426	1.500	1.463	0.987	236	-5
pyrazine	2,5	[C,C]	2.670	1.492	1.524	1.508	0.965	176	19
	1,4	[N,N]	2.817	1.423	1.423	1.423	1.015	309	26
pyridazine	2,5	[C,C]	2.666	1.522	1.522	1.522	0.961	169	9
	1,4	[C,N]	2.770	1.418	1.545	1.482	0.975	222	-37
1,2,3-triazine	3,6	[C,C]	2.650	1.514	1.514	1.514	0.955	177	23
	1,4	[C,N]	2.686	1.452	1.497	1.475	0.951	199	-55
1,2,4-triazine	2,5	[C,N]	2.738	1.423	1.535	1.479	0.953	187	-79
	1,4	[N,N]	2.776	1.384	1.451	1.418	0.999	263	-36
	2,5	[C,N]	2.700	1.446	1.504	1.475	0.958	191	-67
1,3,5-triazine	3,6	[C,C]	2.597	1.507	1.524	1.516	0.931	152	4
	1,4	[C,N]	2.671	1.446	1.443	1.445	0.979	215	-21
1,2,4,5-tetrazine	3,6	[C,C]	2.534	1.523	1.523	1.523	0.906	125	-16

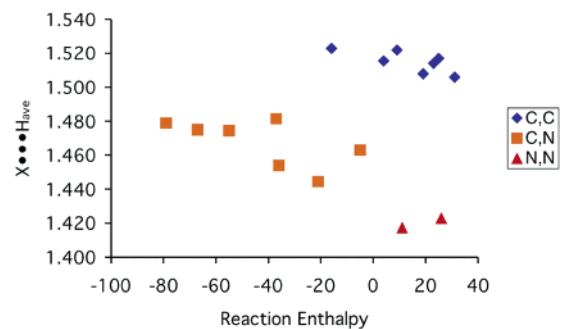
^a X1 and X2 are the two atoms being hydrogenated, and the atoms are numbered from the bottom in an anticlockwise manner. ^b Distance between the X1 and X2 atoms in the ground state of the substrate. ^c Distance between the reacting atoms in the TS. ^d Average of X1-H and X2-H distances.

**Figure 12.** Calculated barriers versus reaction enthalpies for the 1,4-hydrogenations of (hetero)aromatic molecules (0 K, kJ mol⁻¹).

and carbon center, respectively, and we refer to this type of reaction consequently as [C,N] hydrogenation. In a similar manner, the 1,4-hydrogenation of pyridine at C2 and C5 is of the [C,C] type. The results for the 1,4-hydrogenation reactions in these and other simple (six-membered-ring) aromatic and heteroaromatic molecules are summarized in Table 4.

The barriers are plotted against the reaction enthalpies in Figure 12. A quick perusal shows that there is no trivial correlation between the barrier and the reaction enthalpy that can account for *all* the reactions. However, it is evident that among the [C,C]-type hydrogenations, there is a reasonable linear barrier/enthalpy correlation ($R^2 = 0.91$), consistent with the Bell–Evans–Polanyi (BEP) principle.²⁷ Separate correlations between the barriers and the reaction enthalpies are observed for the [C,N]- and [N,N]-type hydrogenations. It appears that, among each group of hydrogenations, the relative magnitudes of the barrier are largely determined by the relative reaction enthalpies.

We note that hydrogenations involving N-centers have higher barriers than those that involve only C-centers in these cyclic systems. A possible explanation is associated with nitrogen being more electronegative than carbon, which would lead to more

**Figure 13.** Calculated distance between the reacting heavy and hydrogen atoms ($X\cdots H_{ave}$, Å) in the TS versus the reaction enthalpy (0 K, kJ mol⁻¹).

contracted nitrogen π -type orbitals than those for the corresponding carbon analogues. In the 1,4-hydrogenation reactions, this may result in less efficient orbital overlap in the transition structure between nitrogen and hydrogen than between carbon and hydrogen and, hence, contribute to a higher reaction barrier. This effect appears to be more prominent when comparing [C,C]- and [C,N]-hydrogenations versus [C,N]- and [N,N]-hydrogenations.

Figure 13 displays a plot of the average of the X1...H and X2...H distances ($X\cdots H_{ave}$) in the TS against the reaction enthalpy, where X1 and X2 are the atoms being hydrogenated. Among the [C,C]-hydrogenations, we can see that the $X\cdots H_{ave}$ distance tends to decrease as the reaction enthalpy increases. This is consistent with the Hammond postulate,²⁸ with $X\cdots H$ bond formation becoming more complete in the TS as the reaction becomes less exothermic (or more endothermic). A similar pattern is also observed for the [C,N]-hydrogenations.

As noted previously, the benzene ring in the transition structure for the uncatalyzed 1,4-hydrogenation of benzene (Figure 9) has developed significant “boat” character, and the H...H distance is also perturbed significantly from its initial value. What are the energy costs for such distortions? We have

(27) (a) Bell, R. P. *Proc. R. Soc. London, Ser. A* **1936**, *154*, 414. (b) Evans, M. G.; Polanyi, M. *Trans. Faraday Soc.* **1938**, *34*, 11.

(28) Hammond, G. S. *J. Am. Chem. Soc.* **1955**, *77*, 334.

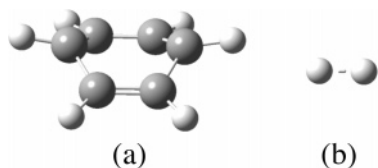


Figure 14. Components of the transition structure for the uncatalyzed 1,4-hydrogenation of benzene: (a) benzene at TS geometry, and (b) H₂ at TS geometry.

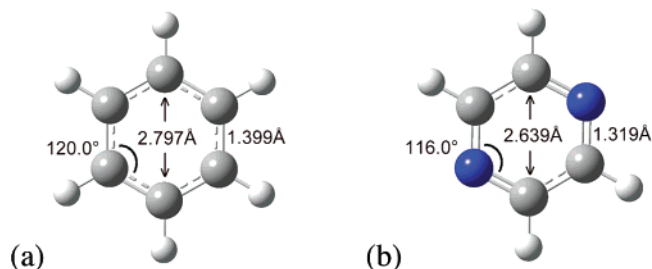


Figure 15. Selected structural parameters for (a) benzene and (b) pyrazine.

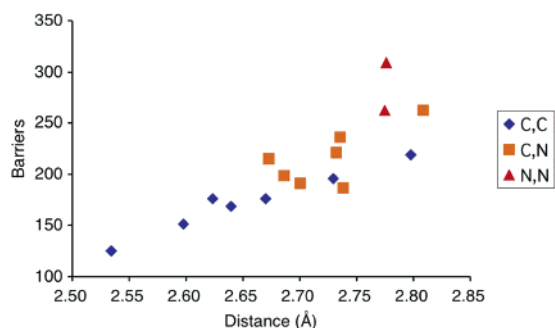


Figure 16. Reaction barriers versus distance between substrate atoms being hydrogenated (d_{ring} , Å) for the uncatalyzed 1,4-hydrogenation of benzene and heteroaromatic systems.

estimated the ring and H₂ distortion energies by partitioning the optimized transition structure into two components (Figure 14), namely the aromatic ring and the hydrogen molecule. The single-point energies of the two components were calculated individually, and the single-point energies of the corresponding optimized ground-state reactants were subtracted from the results. The resulting energy differences are then regarded as reasonable approximations to the ring and H₂ distortion energies.

For benzene, the ring and H₂ distortion energies calculated in this manner are 186 and 76 kJ mol⁻¹, respectively. Similarly, the corresponding values for the [C2,C5]-hydrogenation of pyrazine are 161 and 56 kJ mol⁻¹, respectively. Thus, in both cases the total distortion energy is dominated by the ring distortion energy. In order to rationalize the differences in distortion energies observed for the seemingly similar heteroaromatics, a closer examination of the ring geometries is required.

We note that calculated C–N and N–N bond lengths within prototypical aromatic systems are 1.340 Å (pyridine) and 1.308 Å (pyridazine), respectively, which are significantly smaller than the C–C bond length in benzene (1.399 Å). In addition, the ∠C–N–C bond angle is consistently narrower than the ∠C–C–C bond angle, as the nitrogen possesses a lone pair of electrons as opposed to a bonding electron pair on the carbon. Hence, aromatic systems with nitrogen heteroatoms adjacent to the atoms involved in 1,4-hydrogenation are expected to have a relatively shorter distance between the reacting atoms in the TS (d_{ring}) for these atoms. For example, the d_{ring} distance

corresponding to the 2,5-positions of pyrazine (Figure 15b) is shorter than that of benzene (Figure 15a) by 0.158 Å. This is because of its two adjacent C–N bonds (1.340 Å) as opposed to the relatively longer C–C bonds (1.399 Å) of benzene, as well as the narrower ∠C–N–C bond angle (116.0°) relative to the ∠C–C–C bond angle (120.0°) of benzene. This reduction in the ground-state d_{ring} value may be a reason behind the lower distortion energies for the [C2,C5] hydrogenation of pyrazine compared with that for benzene and may also contribute to the lower hydrogenation barrier. A plot of barrier versus d_{ring} indeed reveals that the barriers for [C,C]-type 1,4-hydrogenation reactions vary with d_{ring} in an approximately linear manner ($R^2 = 0.95$) (Figure 16). This correlation potentially allows the 1,4-hydrogenation barriers to be estimated from a *ground-state* geometric property, which is quite a remarkable result.

4. Conclusions

Quantum chemistry calculations have been applied to the study of the uncatalyzed and catalyzed 1,2- and 1,4-hydrogenation reactions of simple conjugated and aromatic systems. The following important points emerge from the present study:

1. For each substrate studied, the uncatalyzed 1,4-hydrogenation barrier is found to be markedly lower than the uncatalyzed 1,2-hydrogenation barrier, despite similar reaction enthalpies. The differences in 1,4- and 1,2-hydrogenation barriers are consistent with orbital symmetry considerations, whereby the 1,4-hydrogenation is regarded as a [4 + 2]-type cycloaddition and hence is symmetry allowed, while 1,2-hydrogenation belongs to the class of [6 + 2]-type cycloadditions and is formally symmetry forbidden.

2. The HF-catalyzed 1,2-hydrogenation barriers are noticeably lower than the corresponding uncatalyzed 1,2-barriers, while the converse is observed for catalyzed and uncatalyzed 1,4-hydrogenations barriers. This may be attributed to the catalyzed 1,2-hydrogenation being effectively an allowed [6 + 2 + 2]-type cycloaddition (in contrast to the forbidden [6 + 2] reaction). In the case of 1,4-hydrogenation reactions, the (constrained) catalyzed reaction is of the [4 + 2 + 2]-type, which is formally symmetry forbidden while the uncatalyzed 1,4-hydrogenation is of the symmetry-allowed [4 + 2] type.

3. The H₂-catalyzed 1,2-hydrogenation reaction has a lower barrier than many of the acid-catalyzed 1,2-hydrogenations. The remarkable effect of H₂ catalysis is attributed to more efficient orbital overlap for the synchronous H₂-catalyzed reaction.

4. Orbital symmetry considerations are found to be less important for substrates with lower symmetry (e.g., acrolein and propenimine). In these cases, the presence of the HF catalyst slightly lowers the 1,4-hydrogenation barrier, in contrast to the increase expected on the basis of orbital symmetry considerations. The effect of substituents on the barriers is found to be relatively small.

5. The uncatalyzed 1,2-hydrogenation transition structures are similar in shape to that for the 1,2-hydrogenation of ethene. The transition structure for the catalyzed 1,2-hydrogenations of benzene are also similar to those for the catalyzed 1,2-hydrogenations of ethene. In addition, the structural parameters vary with change in catalyst in a similar manner for the two reactions.

6. The barrier for the catalyzed 1,2-hydrogenation of benzene correlates well with the acidity of the corresponding catalyst.

Separate correlations are observed for the first-row and second-row catalysts. In a similar manner, a correlation between the acidity of the catalyst and the reaction barrier is found for the 1,4-hydrogenation reactions with the more acidic catalysts. These observations are similar to those found previously for the catalyzed 1,2-hydrogenation of ethene and are suggestive of competing factors, such as catalyst acidity and basicity, being involved in the catalytic process.

7. The 1,4-hydrogenation of simple heteroaromatic molecules containing one or more nitrogen heteroatom(s) is found to be qualitatively similar to the 1,4-hydrogenation of benzene in terms of both barrier and transition structure. We find that the barriers for a given type of reaction ([C,C], [C,N], or [N,N]) are related to the reaction enthalpy by the Bell–Evans–Polanyi principle. In addition, [C,C]-type hydrogenations generally have lower barriers than either the [C,N]- or [N,N]-type hydrogenations.

8. The energy required to distort the aromatic ring in the transition structure is a key component of the barrier. This ring distortion energy is found to correlate with the distance across the ring that is required to be spanned by the reacting H₂ (termed d_{ring}). Larger d_{ring} values correspond to greater hydrogenation barriers. The correlation between these two quantities enables the [C,C]-type 1,4-hydrogenation barriers to be predicted from a ground-state property.

Acknowledgment. We gratefully acknowledge generous allocations of computing time from the National Facility of the Australian Partnership for Advanced Computing (APAC), the Australian National University Supercomputing Facility (ANUSF) and the Australian Centre for Advanced Computing and Communications (AC3), the award (to G.Z.) of a University of Sydney Summer Research Scholarship, the provision (to B.C.) of a New Zealand Science & Technology Postdoctoral Fellowship by the Foundation for Research, Science & Technology, and the award (to L.R.) of an Australian Research Council Discovery Grant and funding from the ARC Centre of Excellence in Free Radical Chemistry and Biotechnology. We thank Dr Stefan Senger for some preliminary calculations.

Supporting Information Available: GAUSSIAN 03 archive entries for B3-LYP/6-31+G(d)-optimized geometries of relevant equilibrium structures and transition structures, calculated MPWB1K/6-311+G(3df,2p) total energies, calculated G3-(MP2)-RAD energies for selected species and reactions, and the full citation for ref 10. This material is available free of charge via the Internet at <http://pubs.acs.org>.

JA066251A